ISSN: 2754-6705

Journal of Mathematical & Computer Applications

SCIENTIFIC Research and Community

Research Article

Open Access

Basic Investigation on the Electrical Structure Characteristics of 72 V Battery Charging Connector

Sang Won Seo[1], Dong Jin Kim[2] and Kyung Hoon Jang[3*]

[1]SUNKWANG LTI (Seoul, Gwanak-gu, Nabugunhwan-ro 1702, Songsan Building 3rd Floor), Korea

[2]SUNKWANG LTI (Seoul, Gwanak-gu, Nabugunhwan-ro 1702, Songsan Building 3rd Floor), Korea

[3]Korea Conformity Laboratories(199, Gasan digital 1-ro, Geumcheon-gu Seoul, 08503, Korea

ABSTRACT

This paper presents a numerical study of a 72-V battery-charging connector, covering electric-field distribution, abnormal 8/20 μs surge current, and transient current during internal short circuits. The connector geometry conforms to KS R 6100-2:2024. While the broader project combines testing and simulation to assess structural and electrical performance, this paper focuses on the simulation methodology and results. Two excitation models are employed: (i) a double-exponential function that reproduces the 8/20 μs surge waveform specified in KS R 6100-2 and (ii) an exponential rise-decay model that approximates the transient current during an internal short circuit. Electric-field calculations use Maxwell's equations under a quasi-static assumption, reduced to Poisson's equation for the scalar potential. Based on the analysis, we propose targeted modifications aD design improvements to the standardized terminal and present an optimized connector model.

***Corresponding author**

Kyung Hoon Jang, Korea Conformity Laboratories(199, Gasan digital 1-ro, Geumcheon-gu Seoul, 08503, Korea.

Received: July 21, 2025; **Accepted:** October 28, 2025, **Published:** November 03, 2025

Keywords: Finite Element Method, Electric Field Analysis, Battery Charging Terminal, Numerical Analysis, Optimized Design

Introduction

With the rapid development of the electric vehicle and battery industries, the electric vehicle charging connector, which is a key component in power transmission, plays a crucial role in charging systems [1]. The primary roles of a battery charging connector include the efficient transmission of current and voltage with minimal losses and temperature rise, the suppression of resistance increase through the reduction of contact resistance and thermal management to disperse heat generated at the contact interface and prevention discharge and tracking by optimized insulation design. In other words, the connector's primary purpose lies in ensuring a robust electrical connection between the charging infrastructure and the vehicle, thereby supporting the consistent and efficient transfer of high-power [2].

For the insulation design of battery charging connectors, electric field analysis, abnormal surge current and internal short-circuit transient current are critical factors that significantly influence the performance and reliability of the connector. If insulation design does not sufficiently account for factors several critical issues may arise. Excessive field concentrations can initiate partial discharges or dielectric breakdown, thereby accelerating the degradation of insulating materials. Furthermore, inadequate consideration of transient and surge current phenomena may induce localized overheating, carbonization, or surface tracking, which in turn diminishes effective creepage and clearance distances. These failure mechanisms ultimately compromise the electrical and mechanical integrity of the charging connector and may lead to severe safety risks, including fire hazards and complete system failure [3-5].

Recently, a lot of work has been devoted to improving the safety design of battery charging connectors and to analyzing failures under abnormal surge current conditions. Meyer et al., reviewed the accelerated aging of insulation materials exposed to fast, repetitive voltages, highlighting the impact of high slew-rate switching in wide bandgap (WBG) converter systems and suggesting critical challenges and directions for future research [6]. Jin et al., investigated the electro-thermal behavior of power battery connectors using an ANSYS based finite element model, focusing on how connector thickness influences the temperature distribution and thermal reliability [7]. Lin et al., developed a thermal circuit and numerical simulation model for EV charging connectors, analyzing the effects of insulation length, material properties and housing design on heat dissipation and temperature rise [8]. Risdiyanto et al., investigated the thermal distribution of Li-ion battery connectors by combining experiments and simulations, and suggested that surface coating and reduced contact resistance significantly improve thermal performance [9]. Liang et al., proposed a CFD-based prediction method for EV connector temperatures, demonstrating that their model can accurately forecast heat accumulation under various operating conditions [10].

In this paper, we have focused on the behavior of electric field, abnormal surge current and internal short-circuit transient current

for verification of 72 V battery charging connector. To verify the structural and electrical performance of the battery charging connector using the electric currents module, two current models were applied to analyze the electrical behavior of the battery charging connector.

Simulation Setup

The numerical simulation for verification of 72 V battery charging connector was carried out using the electric currents module. For the analysis, two current models (abnormal surge current and internal short-circuit transient current) were applied, these basic equations are presented as follows:

This equation represents the surge current waveform with a double exponential form, typically applied to reproduce the standardized 8/20 μs surge current. It describes a waveform where the current rises sharply at the beginning and then decays exponentially. This model is widely used in accordance with IEC 61000-4-5 to represent surge current transients.

$$I(t) = I_{surge} \cdot \frac{e^{-\alpha t} - e^{-\beta t}}{e^{-\alpha t_{pk}}} \cdot flc2hs(t, dHH) \quad (1)$$

Where the subscripts α and β denote fast exponential decay constant and slow exponential decay constant, respectively; I_{surge} is the peak surge current amplitude, tpk is time to peak current; *flc2hs*(*t, dHH*) is the Heaviside step function used in simulations to control waveform initiation; *DHH* is delay or smoothing parameter for the step function.

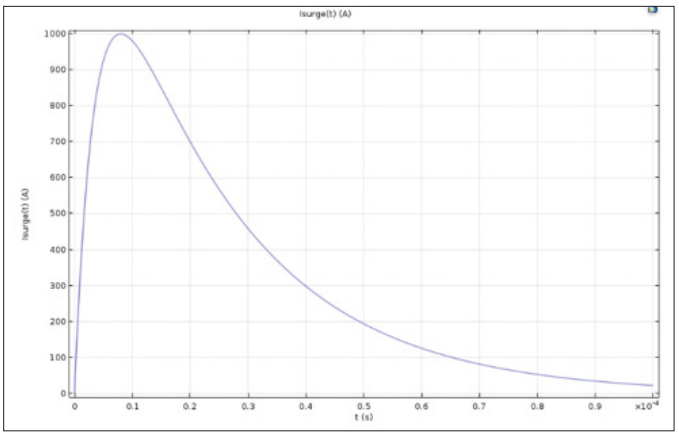

Figure 1: Typical 8/20 μs Surge Waveform

In the case of internal short-circuit transient current, this equation represents the transient current generated during an internal short-circuit, the waveform initially exhibits a rapid exponential rise, followed by a slower exponential decay. It reflects the simplified transient response of a real short-circuit event, making it suitable for numerical simulations.

$$I(t) = I_{peak} \cdot \left(1 - e^{-\frac{t-t0}{tr}}\right) \cdot e^{-\frac{t-t0}{tf}} \cdot flc2hs(t - t0, dH) \quad (2)$$

Where I_{peak} peak short-circuit current amplitude; *t0*, *tr* and *tf* denote initial time when the short-circuit occurs, rise time constant and fall time constant, respectively; *dH* is delay or smoothing parameter for the step function; *flc2hs*(t-t_0, *dH*) is heaviside step function ensuring current initiation at t_0.

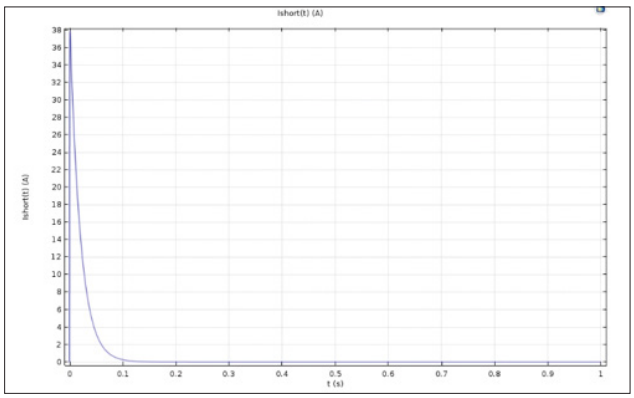

Figure 2: Typical Transient Current Waveform

In electric field analysis, the governing equations are derived from Maxwell's relations. The charge density ρ is expressed as

$$\text{div } D = \rho_{charge\ density} \quad (3)$$

where D=εE (4) and E=-∇V (5). Combining Equations (3)-(5), the general form of Poisson's equation for the electric field can be written as

$$\text{div } \varepsilon_r \cdot (-\nabla E) = \rho_{space\ charge} \quad (6)$$

Here, ε_r denotes the relative permittivity of the material, and ρ represents the space charge density. In this study, the space charge density is assumed to be negligible, i.e., ρ=0.

The temporal variation of current density is governed by the continuity equation, which links the current density and bulk charge density as follows:

$$\nabla \cdot J = \frac{\delta \rho_{space\ charge}}{\delta t} = 0 \quad (7)$$

Substituting Equation (5) into Equation (6), the relationship between current density and field strength can be established.

$$\nabla \cdot (J + \varepsilon \frac{\delta E}{\delta t} = 0 \quad (8)$$

Assuming Ohm's law applies, the current density can be expressed as

$$J = \sigma E \quad (9)$$

Where J is the current density, and it can be calculated following Equation (8) from Equations (7)-(9) using Ohm's law as follows:

$$\nabla \cdot (\sigma E) = \nabla \cdot J = 0 \quad (10)$$

Where σ is the electrical conductivity of each material, and the electric field is determined by the conductivity from Equation (10)

By substituting Equation (10) into Equation (7), the current continuity equation can be expressed as Equation (11) and (12) as follows:

$$\nabla \cdot (\sigma E) + \frac{\delta \rho}{\delta t} = 0 \quad (11)$$

$$\nabla \cdot \left(\sigma E + \frac{\delta E}{\delta t}\right) = 0 \quad (12)$$

Since the electric field is the result of the spatial differentiation of the electric potential, it can be expressed as follows:

$$\nabla\cdot(-\sigma\nabla V)=0 \qquad (13)$$

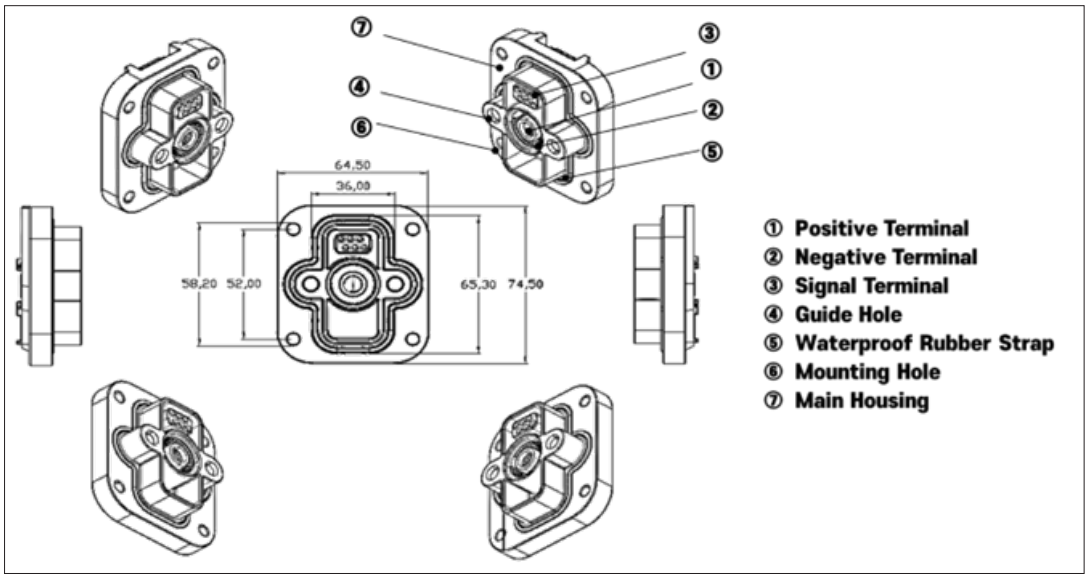

Figure 3: Numerical Model Geometry Of 72 V Battery Charging Connector

Simulation Model Geometry

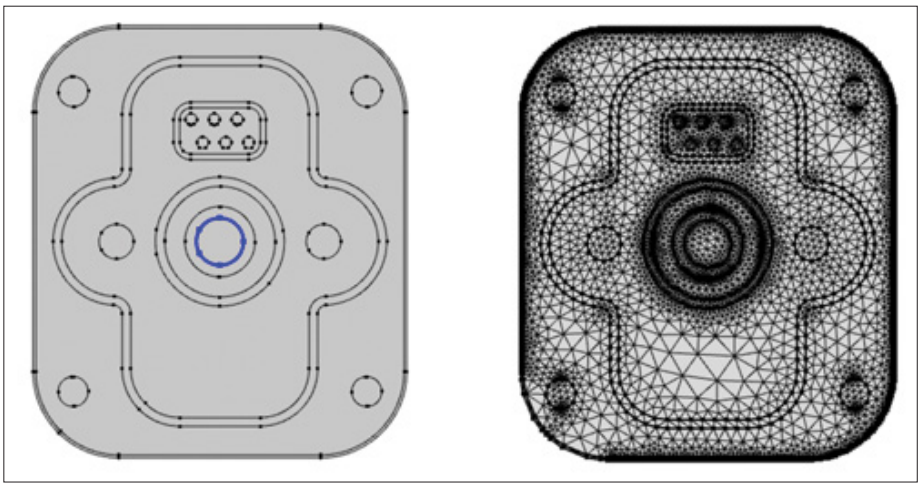

Figure 4: The Simulation Geometry and Mesh Size of the Model

Figure 3 and Figure 4 shown computer aided design representation of the numerical model geometry in COMSOL Multiphysics 2D model. The simulation domain was constructed from a two-dimension of the connector assembly illustrated in the technical drawing. The geometry consists of a central housing structure with four symmetrically arranged contact regions, each incorporating a circular aperture to represent the conductive terminal interface. The outer contour includes rounded edges and mounting features. Dimensional parameters were imported directly from the CAD drawing to maintain fidelity between the physical design and the computational model. Key features such as the terminal holes, outer housing width and geometry was simplified to a 2D cross-sectional representation in order to reduce computational cost while retaining all critical structural details relevant to the simulation. This geometric abstraction allows for precise evaluation of current density, electric field distribution across the connector while minimizing unnecessary computational complexity from the 3-dimensional model.

Table 1: Waveform Function Parameters Used for Each Analysis

Waveform Function			value
Electric Field	V_0	Electric Potential	72[V]
Abnormal Surge Current (8/20 μs)	I_{surge}	Surge Current	500[A]
	Alpha	First Exponential Decay Trate	4.32e4[s^{-1}]
	Beta	Second Exponential Decay Rate	2.74e5[s^{-1}]
	t_{pk}	Time to Peak Current	ln(beta/alpha) / (beta-alpha)
	dHH	Smoothing Width Parameter	2e-6[s]
Internal Short Circuit Transient Current	V_{bat}	Battery Voltage	72[V]
	R_{tot}	Total Resistance	0.05[ohm]
	I_{peak}	Maximum Current	Vbat/Rtot
	t_0	Current Initiation Time	1e-4[s]
Current	t_r	Rise time constant	2e-4[s]
	tr	Decay time constant	2e-2[s]
	dH	Smooth step transition width	2e-5[s]

Table 1 shows summarizes the waveform function parameters applied to the electrostatic analysis, abnormal surge current and internal short-circuit transient current simulation. The electric field defines a constant potential boundary condition, while the surge and short-circuit are modeled using exponential decay functions and transient current waveforms, respectively. Each parameter is denoted by its characteristic time constant, amplitude and smoothing factor corresponding to the physical transient behavior of the system.

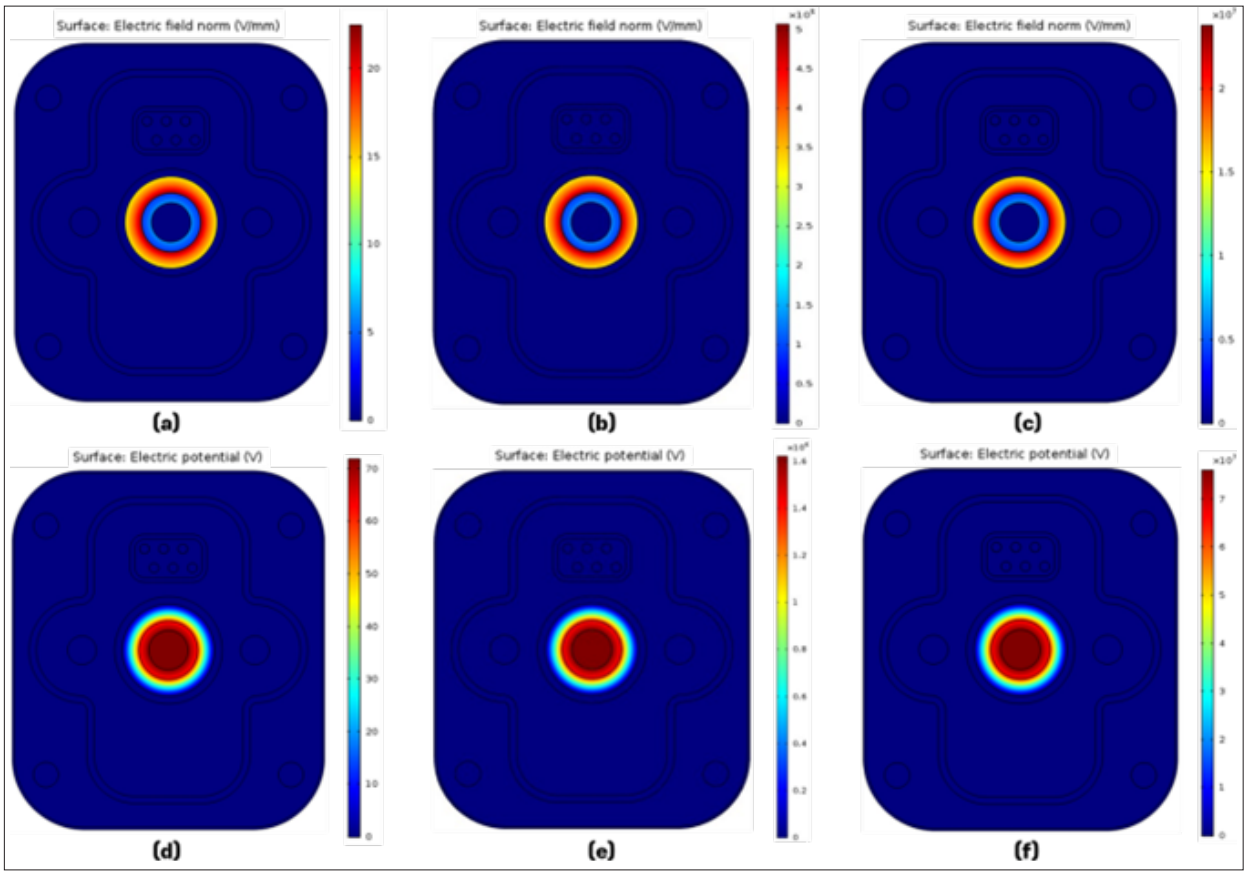

Figure 5: Electric Field and Electric Potential Distributions Obtained from Each Analysis Case

Numerical Analysis Results

The simulation results presented in Figure 5 demonstrate differences in the electric field and potential distributions under each simulation condition. In the normal electrostatic analysis (Figure 5a and 5d), the electric field intensity is symmetrically distributed around the electrode, with a gradual radial decay indicating a stable potential gradient. The field strength remains within a predictable range, suggesting a uniform dielectric environment and minimal distortion in the electric flux path. Under the abnormal surge current condition (Figure 5b and 5e), a notable enhancement in the electric field is observed near the electrode boundary. This localized concentration of electric field implies a sharp rise in potential gradient caused by transient over voltage. In the potential distribution, the equipotential lines are concentrated near the conductor, indicating charge accumulation that can promote the initiation of partial discharge. The internal short-circuit transient current (Figure 5c and 5f) produces an even more pronounced distortion in the electric field distribution. The electric field intensity sharply increases near the short-circuited region, forming a dense gradient zone with asymmetry relative to the positive electrode. This result indicates a significant redistribution of charge density due to internal current flow. The corresponding potential distribution also reveals a steeper voltage drop region, which is consistent with rapid transient current propagation and localized heating phenomena often associated with internal short-circuit events. Figure 6(a)-(f) shown the distributions of electric potential and electric field under three simulation: Figure 6(a) and (d) represent the normal electrostatic analysis, Figure 6(b) and (e) the abnormal surge current condition, and Figure 6(c) and (f) the internal short-circuit transient current condition. In normal electrostatic condition, the potential distribution is symmetrically aligned along the dielectric boundary, indicating a stable and uniform electric field concentrated near the electrode-dielectric interface. The electric field magnitude under $72V$ rated voltage conditions remains within the expected range, showing that the insulation layer and dielectric maintain proper potential gradients without local enhancement. In the case of Figure 6(b) and (e), the electric potential values at the electrode-dielectric and dielectric-air insulation interfaces were found to be 1.6×10^{6} V and 1.4×10^{6} V, respectively. When a surge current of 500 A was applied, electric field concentrations of 1.36×10^{5} V/mm and 5.05×10^{5} V/mm were observed at the electrode-dielectric and dielectric-air insulation interfaces, respectively. In Figure 6(c) and (f), the electric potential values at the electrode-dielectric and dielectric-air insulation interfaces were 7.7×10^{7} V and 6.6×10^{7} V, respectively. Under the internal short-circuit current condition, electric field concentrations of 6.39×10^{6} V/mm and 2.37×10^{7} V occurred at the electrode-dielectric and dielectric-air insulation interfaces, respectively.

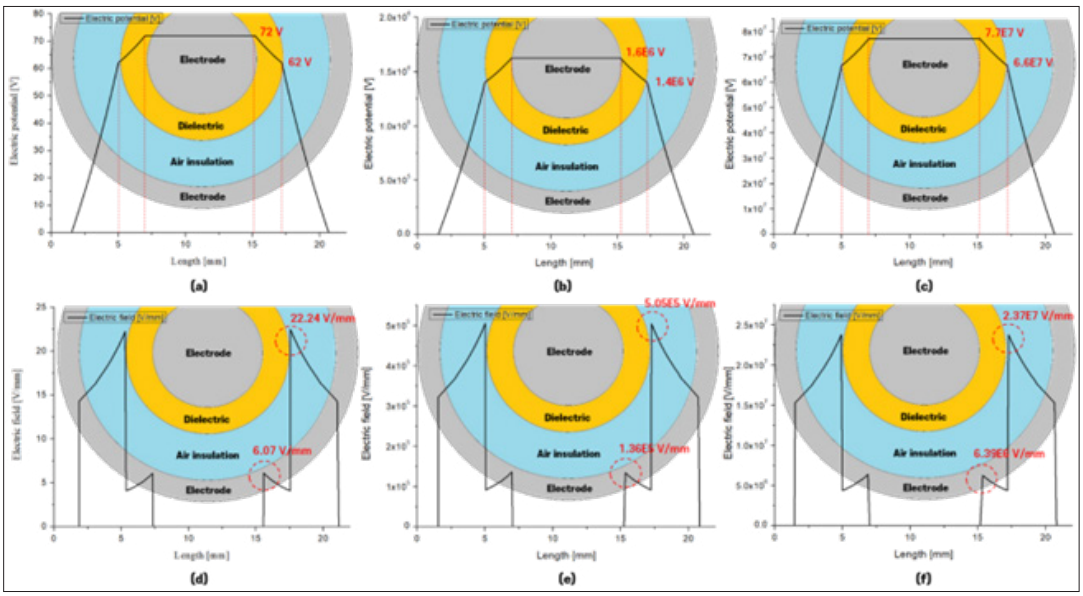

Figure 6: Electric Field and Electric Potential Distributions Obtained from Each Analysis Case

Discussion and Conclusion

This paper conducted an electric field analysis of the 72 V battery charging connector model specified in KS R 6100-2:2024 under both steady-state and transient state, respectively. The results revealed that the electric field was concentrated at the interfaces between the electrode and dielectric, dielectric and air insulation. In particular, during the occurrence abnormal surge currents and internal short-circuit transient current, a sharp increase in the electric field intensity was observed at each interface. The calculated field strength exceeded the dielectric and air insulation breakdown voltage, indicating the potential for electrical discharge. In practice, when such transient fields are momentarily formed, partial discharge may initiate at the interface regions, leading to arc tracking, insulation degradation and in severe cases, flame or explosion induced by arcing. Future work will involve experimental validation of the simulation results, followed by comparative analysis between simulation and test data to establish the optimal design of the battery charging connector.

Acknowledgement

This study was supported by the KETEP (Korea Energy Technology Evaluation and Planning). 20215710100360, development of mobile application product technology using re-manufactured batteries.

References

1. Yannan Li (2025) Thermal Management Optimization for High Power EV Charging Connectors: A Heat Pipe-based Design Approach. Applied Thermal Engineering 279: 127674 -127680.
2. Jigar Sarda (2024) A review of the electric vehicle charging technology impact on grid integration policy consequences challenges and future trends. Energy Reports 12: 5671-5692.
3. Davoud Esmaeil Moghadam (2020) Electrical Insulation at 800 V Electric Vehicles. Conference Proceedings of ISEIM https://www.vonroll.com/app/uploads/2023/03/Electrical-Insulation-at-800-Volt-Electric-Vehicles.pdf.
4. Huan Wang (2025) A Review of Research Progress in Very Fast Transient Overvoltage(VFTO) Suppression Technology. Energies https://www.mdpi.com/1996-1073/18/9/2147.
5. Earl ARL Pannila (2021) Signatures of Transient Overvoltages in Low Voltage Power Systems in Tea Factories and Their Implications on Insulation Deteroration and Allied Power Quality Issues. Journal of Electrical and Computer Engineering https://onlinelibrary.wiley.com/doi/10.1155/2021/2623965.
6. Meyer (2019) Accelerated Insulation Aging Due to Fast, Repetitive Voltages: A Review Identifying Challenges and Future Research Needs. IEEE Transactions on Dielectrics and Electrical Insulation https://ieeexplore.ieee.org/document/8858125.
7. Biao Jin (2022) Temperature Field Simulation and Analysis of Connector for Power Battery. International Conference on Advances in Modern Physics Sciences and Engineering Technology(ICPSET) https://iopscience.iop.org/issue/1742-6596/2242/1.
8. Xueyan LIN (2020) Thermal performance analysis of electric vehicle charging connectors. Thermal Science https://doiserbia.nb.rs/Article.aspx?ID=0354-98362000313L.
9. Agus Risdiyanto (2016) Experimental and Simulation Studies of Thermal Distribution on Modified Connector of Li-Ion Battery for Electric Vehicles Application. International Journal of Electrical and Computer Engineering (IJECE) https://ijece.iaescore.com/index.php/IJECE/article/view/1131.
10. Yinghuai Liang (2025) A temperature prediction method for electric vehicle charging connectors using a CFD-based deep learning model. International Journal of Thermal Sciences 218: 110120-110139.